Journal of the Egyptian Mathematical Society 25 (2017) 79–85

Contents lists available at ScienceDirect

Journal of the Egyptian Mathematical Society

journal homepage: www.elsevier.com/locate/joems

Original Article

Melting heat and mass transfer in stagnation point micropolar fluid flow of temperature dependent fluid viscosity and thermal conductivity at constant vortex viscosity

Isaac Lare Animasaun

Department of Mathematical Sciences, Federal University of Technology, Akure, Ondo State, Nigeria

ARTICLE INFO

Article history:
Received 7 January 2015
Revised 10 June 2016
Accepted 22 June 2016
Available online 5 July 2016

MSC:
76N20
76D17
76A05
80A20
30E25

Keywords:
Micropolar fluid
Stagnation point flow
Variable viscosity
Variable thermal conductivity
Runge–Kutta Gill
Constant vortex viscosity

ABSTRACT

Steady mixed convection micropolar fluid flow towards stagnation point formed on horizontal linearly stretchable melting surface is studied. The vortex viscosity of micropolar fluid along a melting surface is proposed as a constant function of temperature while dynamic viscosity and thermal conductivity are temperature dependent due to the influence of internal heat source on the fluid. Similarity transformations were used to convert the governing equation into non-linear ODE and solved numerically. A parametric study is conducted. An analysis of the results obtained shows that the flow-field is influenced appreciably by heat source, melting, velocity ratio, variable viscosity and thermal conductivity.

1. Introduction

Within the last few decades, many researchers have reported the behavior of fluid flow within a thin layer formed on a stretchable surface in the presence of pressure gradient. The study of stagnation point flow was pioneered by Hiemenz [1]. Stagnation point flow appears in virtually all fields of science and engineering. Shateyi and Makinde [2] stated that a flow can be stagnated by a solid wall or a stagnation point in the interior of the fluid domain. For more related studies on stagnation point flow, prediction of skin-friction and heat/mass transfer near stagnation regions see Refs. [3–6]. Realistically, during the industrial production of polymer fluids, colloidal solutions and fluid containing small additives; there is often a point where the local velocity of the fluid possesses symmetric stress tensor and micro-rotation of particles is zero. Some fluids possess microstructure and belong to class of fluid with nonsymmetric stress tensor. This kind of fluid consists of rigid, randomly oriented particles suspended in a viscous medium; see Lukaszewicz [7]. Micropolar fluid supports couple stress and distributed body torque which cannot be accurately study by using classical Navier–Stokes equation or the viscoelastic flow models. Eringen in [8,9] started an analysis on the theory of micropolar fluids which provided a mathematical model for its non-Newtonian behavior. Recently, Sandeep et al. [10] adopted the idea and reported the effect of radiation on a stagnation point flow of micropolar fluid over a nonlinearly stretching surface. It is a well-known fact in the field of fluid dynamics that static pressure is highest when the velocity is zero and hence static pressure is at its maximum value at stagnation points. In most cases, engineers in the industry tend to introduce internal heat generation to reduce drag and enhance easy flow of fluid around stagnation point where the velocity is zero. Internal energy generation can be explained as a scientific method of generating heat energy within a body by a chemical, electrical or nuclear process. Natural convection induced by internal heat generation is a common phenomenon in nature. Crepeau and Clarksean [11] carried out a similarity solution for a fluid with an exponentially decaying heat generation term. However, micropolar fluid flow towards a stagnation point on a melting surface is significant. In the presence of space heat source,

E-mail address: anizakph2007@gmail.com

http://dx.doi.org/10.1016/j.joems.2016.06.007

dynamic viscosity and thermal conductivity may certainly vary with temperature whereas the vortex viscosity may never be influenced or influenced infinitesimally.

From the knowledge of kinetic theory of matter, every solid melts if expose to a high temperature. In an earlier study, the effect of melting on heat transfer was studied by Tien and Yen [12]. In recent years, many researchers have investigated and reported the effect of melting parameters. For more details, see Refs. [13–16]. In all of the above mentioned studies, fluid viscosity and thermal conductivity was assumed to be constant function of temperature within the boundary layer. However, it is known that the physical properties of the fluid may change significantly when expose to internal generated temperature. For lubricating fluids, heat generated by the internal friction and the corresponding rise in temperature affect the viscosity of the fluid and so the fluid viscosity can no longer be assumed constant. In a case of melting as reported by many researchers; it is important to notice that temperature of fluid layers at free stream may also have significant effect on the intermolecular forces of the micropolar fluid. The increase of temperature may also leads to a local increase in the transport phenomena by reducing the viscosity across the momentum boundary layer and so the heat transfer rate at the wall may also be affected greatly. According to Refs. [17,18] and Meyers et al. [19], it is a well-known fact that properties of fluid which are most sensitive to an increase in temperature are viscosity and thermal conductivity. Considering this concept, effects of temperature-dependent viscosity and variable thermal conductivity on unsteady MHD flow past an impulsively started vertical surface and MHD non-Darcy mixed convective diffusion of species over a stretching sheet was considered in [20,21]. Motivated by all the works mentioned above, it is of interest to extend the work of [4,22,23] by including such effects on the flow and also consider the diffusion of species (mass) in micropolar fluid flow over a melting surface. This is to further examine a case in which the vortex viscosity of micropolar fluid is negligibly influenced due to the nature of wall temperature in the case of melting heat transfer.

2. Problem formulations

Steady laminar incompressible flow, heat and mass transfer of a micropolar fluid towards a horizontal linearly stretching melting surface is considered. It is assumed that the temperature of the melting surface is T_m while the temperature in the free-stream is T_∞ such that $T_m < T_\infty$. Consequently, the species/mass of the micropolar fluid at the melting wall C_m and at the free stream C_∞ satisfies $C_m < C_\infty$. The temperature and concentration of the solid far from the interface is $T_o(<T_m)$ and $C_o(<C_m)$ respectively. The x-axis is along the melting surface while y-axis is normal to it. It is assumed that the stretching of fluid layer at the free stream (i. e. region of inviscid) is $u_e \to ax$ and stretching velocity of the melting surface $u_w = cx$ where both a and c are known as stretching index with unit s^{-1}. Positive values of a and c corresponds to stretching of the surface while x measures the distance along the surface of the plate. Two equal and opposite forces are introduced along x-axis so that the horizontal melting wall is stretched keeping the origin fixed. This external force induces the fluid to flow in x direction. According to Sir Isaac Newton, the differential form of viscous forces

$$\tau^* = \frac{F}{A} = \mu\frac{\partial u}{\partial y}.$$

Where the local shear velocity is $\frac{\partial u}{\partial y}$ and μ is known as constant of proportionality. Since $\tau^* = \mu\frac{\partial u}{\partial y}$, this formulae assumes that the fluid satisfies all the conditions of Couette flow along a parallel lines and y axis perpendicular to the flow, points in the direction of maximum shear velocity. Upon using the scaling analysis (order of magnitude) according to Ludwig Prandtl, this often leads to the simplification of the remaining viscous term of momentum equation as

$$\frac{\mu}{\rho}\frac{\partial^2 u}{\partial y^2} = \frac{1}{\rho}\frac{\partial}{\partial y}\left(\mu\frac{\partial u}{\partial y}\right) \tag{1}$$

when investigating a case in which viscosity of the fluid flow vary with temperature due to the correlation between the two concepts (i.e. variation of viscosity due to pressure gradient as in the case of Couette flow and variation of viscosity due to temperature). In a case of micropolar fluid where the addition of dynamic viscosity and vortex viscosity plays important role in the modeling of deviatoric stress tensor, it may not be realistic to impose the same condition as in Eq. (1) on the fluid flow over a melting surface. Likewise, it may not be valid to neglect the influence of temperature on the dynamic viscosity of micropolar fluid. It is very important to note that base on this fact, the vortex viscosity might not be influenced the same way with dynamic viscosity. A vortex is a region in a fluid medium in which the flow is mostly rotating around an axis line, the vortical flow that occurs either on a straight axis or a curved axis Loper [24] and Ref. [18]. Examples include whirlpools in the smoke rings, dust devil, wake of a boat, paddle or aeroplane. It is important to also note that both vortex and rotation of micro-elements may be restrained near the wall which possesses low heat energy. In view of this, vortex viscosity is assumed to be constant function of temperature. There are several models for shear viscosity e.g. exponential model, Arrhenius model, Williams Landel–Ferry model, Masuko–Magill model and Batchelor model. All these models were developed for either liquid or gases in which vortex viscosity is zero or totally neglected or out of consideration. Under the usual boundary-layer approximations, the basic equations taking into account the presence of internal heat generation in the energy equation for a micropolar fluid can be written as

$$\frac{\partial u}{\partial x} + \frac{\partial v}{\partial y} = 0, \tag{2}$$

$$u\frac{\partial u}{\partial x} + v\frac{\partial u}{\partial y} = u_e\frac{\partial u_e}{\partial x} + \frac{1}{\rho}\frac{\partial}{\partial y}\left(\mu(T)\frac{\partial u}{\partial y}\right) + \frac{\tau}{\rho}\frac{\partial^2 u}{\partial y^2} + \frac{\tau}{\rho}\frac{\partial N}{\partial y} - \left(\frac{\mu+\tau}{\rho\delta}\right)(u_e - u), \tag{3}$$

$$u\frac{\partial N}{\partial x} + v\frac{\partial N}{\partial y} = \frac{\gamma^*}{\rho j}\frac{\partial^2 N}{\partial y^2} - \frac{\tau}{\rho j}\left(2N + \frac{\partial u}{\partial y}\right), \tag{4}$$

$$u\frac{\partial T}{\partial x} + v\frac{\partial T}{\partial y} = \frac{1}{\rho C_p}\frac{\partial}{\partial y}\left(\kappa(T)\frac{\partial T}{\partial y}\right) + \frac{\kappa(T)a}{C_p\mu(T)}[A^*(T_\infty - T_m)e^{-y\sqrt{\frac{a}{\vartheta}}} + B^*(T - T_m)], \tag{5}$$

$$u\frac{\partial C}{\partial x} + v\frac{\partial C}{\partial y} = D_m\frac{\partial^2 C}{\partial y^2}. \tag{6}$$

The appropriate boundary conditions on velocity, micro-rotation and temperature are

$$u_w = cx, \quad \kappa(T)\frac{\partial T}{\partial y} = \rho[\lambda^* + c_s(T_m - T_o)]v(x,0),$$
$$N = -m_o\frac{\partial u}{\partial y}, \quad T = T_m, \quad C = C_m \quad at \quad y = 0, \tag{7}$$

$$u_e \to ax, \quad N \to 0, \quad T \to T_\infty, \quad C \to C_\infty \quad as \quad y \to \infty. \tag{8}$$

The formulation of $\kappa(T)\frac{\partial T}{\partial y} = \rho[\lambda^* + c_s(T_m - T_o)]v(x,0)$ in Eq. (7) states that the heat conducted to the melting surface

is equal to the heat of melting plus the sensible heat required to raise the solid temperature T_o to its melting temperature T_m. The boundary conditions for gyration N following Ref. [25] indicates that in the neighborhood of the boundary the only rotation is due to the fluid shear and therefore gyration vector must be equal to angular velocity (i. e. $m_o = 0.5$ indicates the vanishing of anti-symmetric part of the stress tensor and denotes weak concentrations). Following the work of Ref. [22], spin gradient viscosity and micro-inertia per unit mass is defined as

$$\gamma^* = \left(\mu + \frac{\tau}{2}\right), \quad j = \frac{\mu}{\rho a}. \tag{9}$$

This assumption is invoked to allow the field of equations predict the correct behavior in the limiting case when the microstructure effects become negligible and the total spin N reduces to the angular velocity [22,25]. Also, temperature dependent variable fluid viscosity model was also built on the condition that $T_w > T_\infty$. Since the temperature of the surface is equivalent to the melting temperature which is very small, it is realistic to assume that vortex viscosity is negligibly influenced by temperature. Hence, the mathematical model of temperature dependent viscosity model used by Mukhopadhyay [26] which was developed using the experimental data of [18] together with the mathematical model of temperature dependent thermal conductivity model of Charraudeau [27], used in [28] which have been modified following the discourse presented in Animasaun [29] as

$$\mu(T) = \mu^*[\aleph_1 + \hbar_1(T_\infty - T)], \quad \kappa(T) = \kappa^*[\aleph_2 + \hbar_2(T - T_m)]. \tag{10}$$

Modification of those mentioned models is necessary due to the melting condition that is incorporated into the mathematical formulation. Also, the influence of temperature on the thermal conductivity of the micropolar fluid during heat conduction in the melting process is properly considered. It is worth mentioning that all models in Eq. (10) are valid in this research since $T_\infty > T_m$. μ^* and κ^* are the constant value of the coefficient of viscosity and thermal conductivity at the freestream respectively. A case where $\aleph_1 = \aleph_2 = 1$ and $(\hbar_1, \hbar_2) > 0$ is considered in this research work. The following relations are now introduced for u and v together with similarity variables

$$u = \frac{\partial \psi}{\partial y}, \quad v = -\frac{\partial \psi}{\partial x}, \quad \eta = y\sqrt{\frac{a}{\vartheta}}, \quad \psi = xf(\eta)\sqrt{a\vartheta},$$
$$N = xa\sqrt{\frac{a}{\vartheta}}g(\eta), \quad \theta = \frac{T - T_m}{T_\infty - T_m}, \quad \phi = \frac{C - C_m}{C_\infty - C_m}. \tag{11}$$

The first two mathematical relations in Eq. (11) satisfy continuity equation Eq. (2). The corresponding modified governing equations of Eqs. (3)–(6) are solved by using the similarity transformations in Eq. (11). The following locally similar ordinary differential equations are obtained:

$$[1 + \xi - \theta\xi + K]\frac{d^3 f}{d\eta^3} - \xi\frac{d\theta}{d\eta}\frac{d^2 f}{d\eta^2} - \lambda[1 + \xi - \theta\xi + K]\left(1 - \frac{df}{d\eta}\right) + f\frac{d^2 f}{d\eta^2} + 1 - \frac{df}{d\eta}\frac{df}{d\eta} + K\frac{dg}{d\eta} = 0, \tag{12}$$

$$\left(1 + \xi - \theta\xi + \frac{K}{2}\right)\frac{d^2 g}{d\eta^2} + f\frac{dg}{d\eta} - g\frac{df}{d\eta} - \frac{K}{[1 + \xi - \theta\xi]}\left(2g + \frac{d^2 f}{d\eta^2}\right) = 0, \tag{13}$$

$$[1 + \varepsilon\theta]\frac{d^2\theta}{d\eta^2} + \varepsilon\frac{d\theta}{d\eta}\frac{d\theta}{d\eta} + P_r f\frac{d\theta}{d\eta} + \frac{[1 + \varepsilon\theta]}{[1 + \xi - \theta\xi]}(A^* e^{-\eta} + B^*\theta) = 0, \tag{14}$$

$$\frac{d^2\phi}{d\eta^2} + S_c f\frac{d\phi}{d\eta} = 0. \tag{15}$$

The dimensionless equations are

$$\frac{df}{d\eta} = \sigma, \quad m[1 + \varepsilon\theta]\frac{d\theta}{d\eta} + P_r f(\eta) = 0, \quad g(\eta) = -0.5\frac{d^2 f}{d\eta^2},$$
$$\theta(\eta) = 0, \quad \phi(\eta) = 0 \ \ at \ \ \eta = 0, \tag{16}$$

$$\frac{df}{d\eta} \to 1, \quad g(\eta) \to 0, \quad \theta(\eta) \to 1, \quad \phi(\eta) \to 1 \ \ as \ \ \eta \to \infty. \tag{17}$$

In Eq. (14), $\theta(\eta) = 0$; it is worth mentioning that the temperature of wall (i.e. horizontal melting stretchable surface) is not at absolute zero since T_m (melting temperature is significant; greater than T_o but less than T_∞. Temperature dependent viscous parameter $\xi = \hbar_1(T_\infty - T_m)$, micropolar coupling constant $K = \tau/\mu$, Porosity parameter $\lambda = \vartheta/\delta a$, temperature dependent thermal conductivity parameter $\varepsilon = \hbar_2(T_\infty - T_m)$, Prandtl number $P_r = C_p\mu/\kappa$, Schmidt number $S_c = \mu/D_m$, velocity ratio parameter $\sigma = c/a$ and melting parameter $m = [C_p(T_\infty - T_m)]/[\lambda^* + c_s(T_m - T_o)]$. The physical quantities of interest (i.e. the local skin-friction coefficient C_f, the dimensionless wall couple stress M_w, the local Nusselt number Nu_x and the local Sherwood number Sh_x) are defined as

$$C_f = \frac{2\tau_w}{\rho(u_e)^2}, \quad C_s = \frac{m_w x}{a\Gamma},$$
$$Nu_x = \frac{xq_w}{\kappa(T_\infty - T_m)} \quad Sh_x = \frac{xL_w}{\kappa(C_\infty - C_m)}. \tag{18}$$

Where Reynold number ($Re_x = \frac{u_e x\rho}{\mu}$), surface shear stress (τ_w), wall couple stress (M_x), the heat transfer from the plate (q_w) and the mass transfer from the plate (L_w) are defined by

$$\tau_w = \left([\mu + \tau]\frac{\partial u}{\partial y} + \tau N\right|_{y=0}, \quad m_w = \left(\Gamma\frac{\partial N}{\partial y}\right|_{y=0},$$
$$q_w = \left(-\kappa\frac{\partial T}{\partial y}\right|_{y=0} \quad L_w = \left(-D_m\frac{\partial C}{\partial y}\right|_{y=0}. \tag{19}$$

Using the similarity variables in Eq. (11), we get

$$0.5C_f\sqrt{Re_x} = [1 + K]f''(0) + Kg'(0), \quad g'(0) = c_s(Re_x)^{-1},$$
$$Re_x^{-1/2}Nu_x = -\theta'(0)$$
$$Re_x^{-1/2}Sh_x = -\phi'(0). \tag{20}$$

3. Numerical method of solution

In this section, the adopted numerical method to solve dimensionless governing equations Eq. (12) to Eq. (15) subject to Eq. (16) and Eq. (17) are discussed. The solutions of the nonlinear boundary valued problem are obtained using Shooting technique with fourth-order Runge–Kutta Gill method. The set of coupled ordinary differential equations along with boundary conditions are converted from BVP to IVP using the method of superposition introduced by Na [30]). The BVP cannot be solved on an infinite interval and it would be impractical to solve it on a very large finite interval. The asymptotic boundary conditions in Eq. (17) as $\eta \to \infty$ are replaced by those at a large but finite value of $\eta = 4$. To integrate the corresponding IVP, $f''(0)$, $g'(0)$, $\theta'(0)$ and $\phi'(0)$ are needed but no such values exist after the non-dimensionalization of the boundary conditions. The suitable guesses values for $f''(0)$, $g'(0)$, $\theta'(0)$ and $\phi'(0)$ were chosen and integration is carried out.

Table 1
Comparison of $f'(0)$ and $-\theta'(0)$ for various values of σ, m and K when $\xi = \lambda = \varepsilon = A^* = B^* = 0$, $S_c = 0$ and $P_r = 1$ with previously published articles.

σ	m	K	Pop et al. [22] $f'(0)$	Pop et al. [22] $-\theta'(0)$	Wang [31] $f'(0)$	Present $f'(0)$
0	0	0	1.232588	−0.570465	1.232588	1.232590614
0	0	1	1.006404	−0.544535		1.006540428
0	1	0	1.037003	−0.361961		1.036768724
5	0	0	−10.264749	−1.396355	−10.26475	−10.264749327

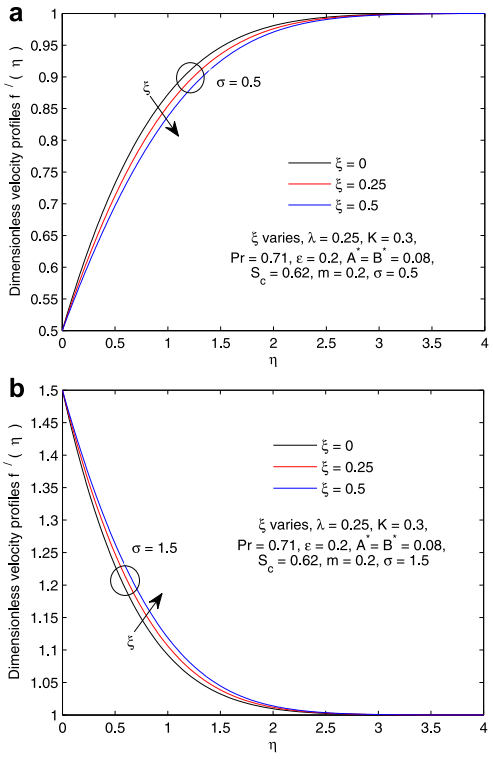

Fig. 1. (a) Dimensionless velocity profiles for various values of ξ when $\sigma < 1$. (b) Dimensionless velocity profiles for various values of ξ when $\sigma > 1$.

The step size is taken as $\triangle\eta = 0.001$. The guess values were adjusted using secant method to give better approximation for the solution. The procedure is repeated until we get the results up to the desired degree of accuracy 10^{-5}.

4. Results and discussions

Using the numerical scheme discussed in the previous section, computation has been carried out for various values of some parameters which are encountered in this research. In order to assess the accuracy of our results, certain results are compared with those reported by Pop et al. [22] and Wang [31] as shown in Table 1, and they are found to be in good agreement. Figs. 1a and 1b depict the variation of velocity distribution at various values of temperature dependent viscous parameter ξ when $\varepsilon = 0.2$, $\lambda = 0.25$, $m = 0.2$, $K = 0.3$, $A^* = B^* = 0.08$, $P_r = 0.71$, $S_c = 0.62$ when velocity ratio parameter $\sigma < 1$ and $\sigma > 1$. It is observed from these figures that the velocity decreases with an increase in ξ when $\sigma = 0.5$. Opposite effect is observed on velocity profiles when σ1.5. In real life, the implication of the velocity ratio parameter σ governing the stagnation flow at $\eta = 0$ can be explained mathematically. When $\sigma = c/a$ and σ is any natural number less than unity; this implies that stretching velocity rate of the horizontal melting wall "c" is less than the stretching rate of fluid layer at free stream "a" (i.e. in the inviscid stream). Due to this reason, the acceleration of the external stream is increased and subdues the effect of parameter ξ which supposed to increase the velocity profiles as the fluid flows along the horizontal melting surface (x−direction). When σ is any natural number greater than unity; this implies that stretching velocity rate of the horizontal melting wall "c" is more substantial than the stretching rate of fluid layer at free stream. This drastically reduces the acceleration of the external stream; hence velocity profile increases with parameter ξ. Physically, the horizontal wall is generating very small amount of heat energy since $A^* = B^* = 0.08$ are internal heat source terms which are to generate thermal energy near the wall and within the fluid domain. At constant vortex viscosity, $\sigma > 1$, $A^* = B^* = 0.08$; when the micropolar fluid heats up, molecules become excited and begin to flow (i.e. intermolecular forces which hold all the fluid molecules so tight is weaken). The energy of this movement is enough to overcome the forces that bind the molecules together, allowing the micropolar fluid to move faster and decreasing its viscosity gradually away from the wall; hence, the velocity increases from the wall to the free stream with an increase in the value of ξ (see Fig. 1b). The effect of temperature dependent dynamic viscosity parameter ξ at a constant vortex viscosity on angular velocity of micropolar fluid (i.e. micro-rotation profile) are displayed in Figs. 2a and 2b) when material parameter $K = 0.3$. From Fig. 2a, it is seen that micro-rotation of particle increases and decreases when $\sigma = 0.5$ and $\sigma = 1.5$ respectively with an increase in magnitude of parameter ξ. This can be traced to the corresponding increase and decrease of the acceleration of the external stream when $\sigma < 1$ ($\sigma = 0.5$) and $\sigma > 1$ ($\sigma = 1.5$) respectively. Typical values for the ratio of viscous diffusion rate to thermal diffusion rate are around 0.05 for mercury, $0.16 - 0.7$ for mixtures of noble gases with hydrogen and around $0.7 - 0.8$ for air and many other gases. Fig. 3a) depicts the effect of temperature dependent thermal conductivity parameter ε on temperature profile $\theta(\eta)$ at various values of P_r. In order to unravel the effect of parameter ε in a case of melting, four cases were considered; in each cases,

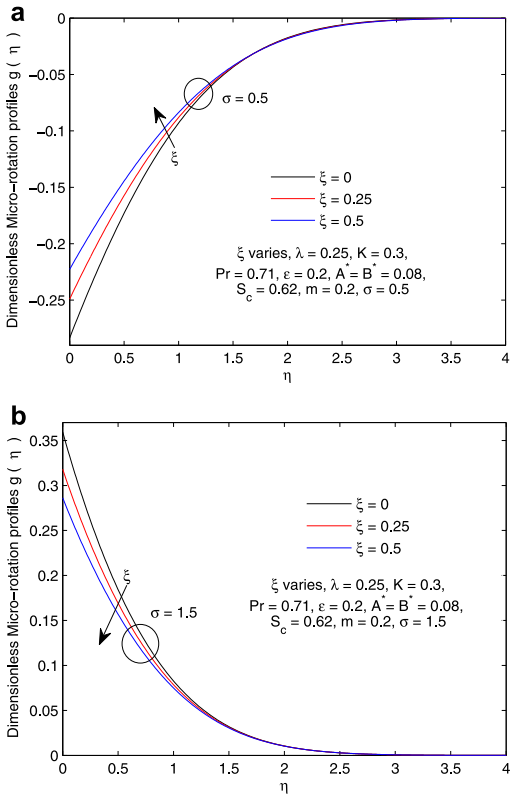

Fig. 2. (a) Dimensionless micro-rotation profiles for various values of ξ when $\sigma < 1$. (b) Dimensionless micro-rotation profiles for various values of ξ when $\sigma > 1$.

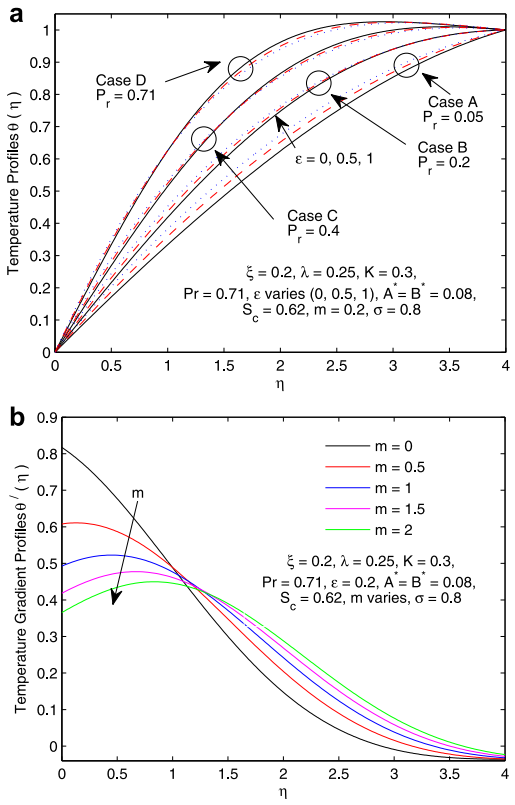

Fig. 3. (a) Dimensionless temperature $\theta(\eta)$ at various values of ε when P_r varies. (b) Dimensionless temperature gradient $\theta'(\eta)$ profiles for various values of melting parameter m.

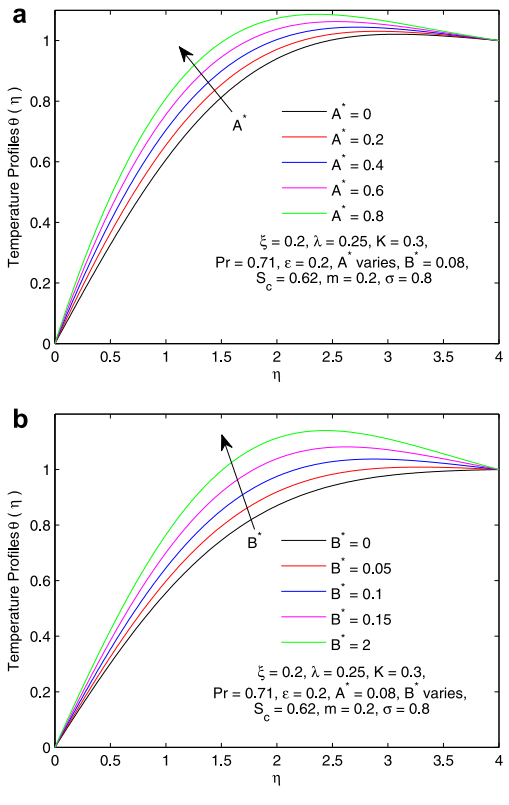

Fig. 4. (a) Dimensionless temperature profiles at various values of space dependent internal heat source parameter A^*. (b) Dimensionless temperature profiles at various values of space dependent internal heat source parameter B^*.

parameter ε increases within $0 \leq \varepsilon \leq 1$. It is observed that when $P_r \ll 1$, temperature profiles increases with η and also with an increase in the magnitude of ε (see case A). It is further observed that with an increase in the magnitude of P_r, the temperature profiles increases near the wall within ($0 \leq \eta \leq 2.4$) and decreases thereafter. To further clarify this strange effect, the magnitude of P_r was further increased. It is observed that $\theta(\eta)$ increases with ε near the wall within the range ($0 \leq \eta \leq 1.35$). When $P_r = 0.71$, the temperature function only increases within a very thin layer near the wall and decreases significantly thereafter till free stream (see case D). This can be explained as follows; at a constant value of C_P, decrease in P_r directly implies increases in thermal conductivity property of the micropolar fluid. This explains the expansion of the thin layer in which temperature increases, as magnitude of P_r decreases with an increase in temperature dependent thermal conductivity parameter, the interval near the wall in which temperature profile increases tends to expand. It is observed that the temperature profile is a decreasing function of melting parameter m while it causes temperature gradient function $\theta'(\eta)$ to decrease near the wall and increase thereafter till free stream (see Fig. 3b). Variation of temperature and concentration for non-Newtonian micropolar fluid with different values of melting parameter m was investigated but not presented herein for brevity. The temperature and concentration profiles are decreasing functions of melting parameter m. Increase in m corresponds to increase in the melting process in which heat energy from the fluid domain is consumed. Due to the correlation between temperature and concentration, the highest concentration is observed at the smallest value of melting parameter. Figs. 4a and 4b depict the influence of the temperature-dependent internal heat generation parameters A^* and B^* on the micropolar fluid in boundary layer. Increase in both parameters leads to an increase in the temperature of the fluid. It is imperative for us to note that an increase in the magnitude of both parameters satisfies the boundary conditions and significantly increases the temperature function with the fluid domain. The local skin friction coefficient of stagnation point micropolar fluid flow over a melting surface ($\frac{0.5C_f\sqrt{Re_x}-Kg'(0)}{[1+K]}$) is plotted against melting parameter at each value of porosity parameter in Fig. 5a. This figure reveals that at each value of λ within $0 \leq \lambda \leq 0.6$, local skin friction coefficient increases with parameter m. Physically, an increase in the magnitude of parameter m corresponds to an increase in the transition rate from solid to liquid. The internal energy of the melting stretchable surface is increased due to the application of heat resulting in a rise of temperature; this tends to reduce the smoothness of the surface and fluid flows very slow. In the same figure, it is noticed that at a given value of parameter m, local skin friction coefficient increases with an increase in λ. It is noticed in Fig. 5b that $Re_x^{-1/2}Sh_x$ decreases with an increase in Schmidt number S_c at any given value of melting parameter m within $0 \leq m \leq 1.4$. The effect of S_c on $Re_x^{-1/2}Sh_x$ is significant when $m = 0$ compared to when $m = 1.4$. The influence of parameter ξ and ε on the local skin friction coefficient $\frac{0.5C_f\sqrt{Re_x}-Kg'(0)}{[1+K]}$, couple stress at the wall $c_sRe_x^{-1}$, Nusselt number $Re_x^{-1/2}Nu_x$ and Sherwood number $(Re_x)^{-1/2}Sh_x$ was investigated. For brevity, this table is not displayed. When $m = \lambda = 0.2$, $\varepsilon = 0$, $K = 0.5$ and $A^* = B^* = 0.1$ it is observed that both $\frac{0.5C_f\sqrt{Re_x}-Kg'(0)}{[1+K]}$ and $c_sRe_x^{-1}$ decreases while $Re_x^{-1/2}Nu_x$ increases with an increase in the magnitude of ξ. It is also noticed that the Sherwood number $(Re_x)^{-1/2}Sh_x$ which is proportional to the local mass transfer rate increases negligible with ξ. It is pertinent to note that the suction at the wall have replaced the melting model. In view of this, the transverse velocity at the wall is of the form $f(0) = -[m\theta'(0)]/[P_r]$. In view of this, an effect of Prandtl number P_r on physical quantities of interest are

Table 2
Values of local skin-friction coefficient $f''(0)$, Couple stress at the wall $g'(0)$, local heat transfer rate $-\theta'(0)$ and local mass transfer rate $-\phi'(0)$ when $\xi = \varepsilon = 0.3$, $\lambda = 0.4$, $K = 0.5$, $A^* = B^* = 0.1$, $S_c = 0.62$, $m = 1$ with various values of P_r when $\sigma < 1$ and $\sigma > 1$.

$P_r \Downarrow$, $\sigma = 0.8$	$f(\eta = 0)$	$f''(\eta = 0)$	$g'(\eta = 0)$	$-\theta'(\eta = 0)$	$-\phi'(\eta = 0)$
0.2	−1.767597181	0.105872879	0.021696964	−0.353519436	−0.114089522
0.4	−1.062013975	0.137686026	0.039300307	−0.424805590	−0.251234714
$P_r \Downarrow$, $\sigma = 1.2$	$f(\eta = 0)$	$f''(\eta = 0)$	$g'(\eta = 0)$	$-\theta'(\eta = 0)$	$-\phi'(\eta = 0)$
0.2	−1.866539137	−0.125470942	−0.033014296	−0.373307827	−0.141300454
0.4	−1.146886946	−0.157679939	−0.054456960	−0.458754778	−0.287663911

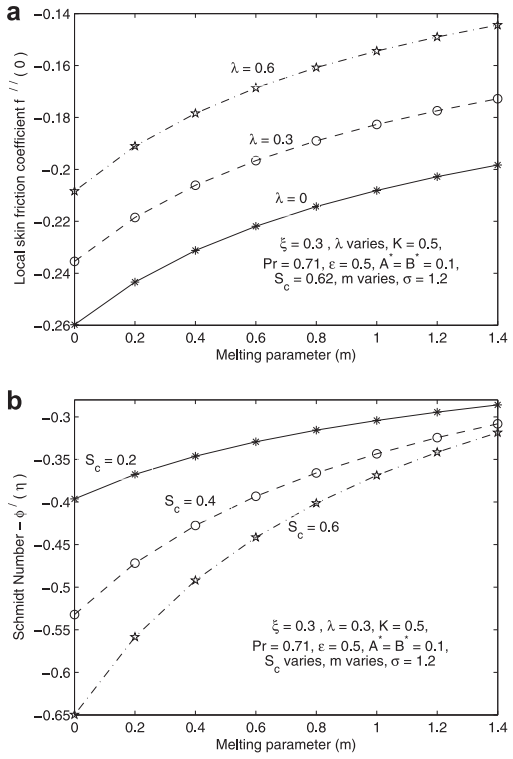

Fig. 5. (a) Local skin friction coefficients $\frac{0.5C_f\sqrt{Re_x}}{1+K}$ against melting parameter m at various values of porosity parameter λ. (b) Sherwood number $(Re_x)^{-1/2}Sh_x$ against melting parameter m at various values of Schmidt number S_c.

highly relevant to Engineers in the industry. Typical variations of the transverse velocity at the wall, local skin friction coefficient, local heat transfer and local mass transfer with increasing values of Prandtl number when velocity ratio parameter $\sigma < 1$ and $\sigma > 1$ is shown in Table 2. It is observed that when $\sigma < 1$ and $\sigma > 1$, the transverse velocity coefficients $(\psi(x,y)/(x\sqrt{a\vartheta})|_{y=0}$ increases with P_r. As magnitude of P_r is increased from 0.2 to 0.6, the percentage increase in transverse velocity coefficients when $\sigma = 0.8$ and $\sigma = 1.2$ are estimated as 53.9% and 52.3% respectively. It is seen in the same table that local skin friction coefficient $(0.5C_f\sqrt{Re_x})/[1+K]$ increases with P_r when $\sigma = 0.8$ and decreases with P_r when $\sigma = 1.2$. In this study, using the stretching velocity ratio $\sigma = 1.2$ implies stretching rate of the fluid layer at the melting wall $c(= 1.2$ or $1)$ is greater than the rate of stretching of the fluid layer at the free stream $a(= 1$ or $0.83333)$. This naturally enhance the fluid flow since $[f'(0) = 1.2] > [f'(\infty) = 1]$. Surprisingly, the velocity function $f'(\eta)$ decreases with P_r while temperature function $\theta(\eta)$ and concentration function $\phi(\eta)$ increases with P_r. The stretching tends to insert a positive pressure which ought to enhance the flow but shear between any two layers in the fluid domain is negatively influenced by increasing the magnitude of P_r. At a constant value of C_P, increase in the magnitude of P_r directly implies decreases in thermal conductivity κ of the fluid; this leads to a decrease in Nusselt number which is proportional to local heat transfer rate $Re_x^{-1/2}Nu_x$ when $\sigma = 1.2$.

5. Conclusion

Steady laminar mixed convection flow, heat and mass transfer of stagnation micropolar fluid flow towards a horizontal linearly stretching sheet taking into account the influence of internal exponentially heat generation and melting is studied considering the variation in fluid viscosity and thermal conductivity due to temperature differences. It can be concluded that local skin-friction coefficient, the dimensionless wall couple stress, the local Nusselt number and the local Sherwood number of the fluid flow problem decrease with an increase in both temperature dependent variable fluid viscosity and thermal conductivity at constant vortex viscosity. An increase in the melting parameter m reduces the temperature gradient profiles of micropolar fluid flow over a melting surface within $0 \leq \eta \leq 0.788$. Temperature and concentration profiles decrease with the increase of melting parameter m. The temperature distribution increases within the fluid domain $(0 \leq \eta \leq 4)$ with an increase in parameter ε only for fluid with $(P_r \ll 1)$. Sherwood number $Re_x^{-1/2}Sh_x$ decreases significantly with Schmidt number when magnitude of melting parameter is small.

Acknowledgments

Thanks are indeed due to the Reviewer(s) for their constructive comments and valuable suggestions which led to a definite improvement of the quality of the manuscript.

References

[1] K. Hiemenz, Die grenzschict neinem in den gleichformigen flussigkeitsstrom eingetauchten geraden kreiszylinder, Dingler's Polytech. J. 326 (1911) 321–410.
[2] S. Shateyi, O.D. Makinde, Hydromagnetic stagnation-point flow towards a radially stretching convectively heated disk, Math. Prob. Eng. (2013), doi:10.1155/2013/616947. Article ID 616947.
[3] O.D. Makinde, Heat and mass transfer by MHD mixed convection stagnation point flow toward a vertical plate embedded in a highly porous medium with radiation and internal heat generation, Meccanica 47 (2012) 1173–1184, doi:10.1007/s11012-011-9502-5z.
[4] K.S. Adegbie, A.J. Omowaye, A.B. Disu, I.L. Animasaun, Heat and mass transfer of upper convected maxwell fluid flow with variable thermo-physical properties over a horizontal melting surface, Appl. Math. 6 (2015) 1362–1379, doi:10.4236/am.2015.68129.
[5] C. Sulochana, N. Sandeep, Stagnation point flow and heat transfer behavior of cu-water nanofluid towards horizontal and exponentially stretching/shrinking cylinders, Appl. Nanosci. (2015) 1–9, doi:10.1007/s13204-015-0451-5.
[6] I.L. Animasaun, C.S.K. Raju, N. Sandeep, Unequal diffusivities case of homogeneous-heterogeneous reactions within viscoelastic fluid flow in the presence of induced magnetic-field and nonlinear thermal radiation, Alexandria Eng. J., in-press (2016), doi:10.1016/j.aej.2016.01.018.
[7] G. Lukaszewicz, Micropolar Fluids: Theory and Applications, Birkhauser, Boston, 1999.
[8] A.C. Eringen, Theory of micropolar fluids, J. Math. Anal. Appl. 16 (1966) 1–18.
[9] A.C. Eringen, Theory of thermomicrofluids, J. Math. Anal. Appl. 38 (1972) 480–496.
[10] N. Sandeep, M.J. Babu, R. Gupta, Effect of radiation and viscous dissipation on stagnation-point flow of a micropolar fluid over a nonlinearly stretching surface with suction/injection, J. Basic Appl. Res. Int. 7 (2015) 73–82.

[11] J.C. Crepeau, R. Clarksean, Similarity solutions of natural convection with internal heat generation, Trans. ASME - J. Heat Transf. 119 (1997) 184–185.
[12] Y.C. Yen, C. Tien, Laminar heat transfer over a melting plate, the modified leveque problem, J. Geophys. Res. 68 (1963) 3673–3678.
[13] N. Bachok, A. Ishak, I. Pop, Melting heat transfer in boundary layer stagnation-point flow towards a stretching/shrinking sheet, Phys. Lett. A 374 (2010) 4075–4079.
[14] A.J. Omowaye, I.L. Animasaun, Upper-convected maxwell fluid flow with variable thermo-physical properties over a melting surface situated in hot environment subject to thermal stratification, J. Appl. Fluid Mech. 9 (4) (2016) 1777–1790.
[15] O.D. Makinde, I.L. Animasaun, Bioconvection in MHD nanofluid flow with nonlinear thermal radiation and quartic autocatalysis chemical reaction past an upper surface of a paraboloid of revolution, Int. J. Therm. Sci. 109 (2016) 159–171, doi:10.1016/j.ijthermalsci.2016.06.003.
[16] O.D. Makinde, I.L. Animasaun, Thermophoresis and Brownian motion effects on MHD bioconvection of nanofluid with nonlinear thermal radiation and quartic chemical reaction past an upper horizontal surface of a paraboloid of revolution, J. Mol. Liq. 221 (2016) 733–743, doi:10.1016/j.molliq.2016.06.047.
[17] I.L. Animasaun, 47nm alumina-water nanofluid flow within boundary layer formed on upper horizontal surface of paraboloid of revolution in the presence of quartic autocatalysis chemical reaction, Alexandria Eng. J. (2016), doi:10.1016/j.aej.2016.04.030. In-press.
[18] G.K. Batchelor, An Introduction to Fluid Dynamics, Cambridge University Press, London, 1987.
[19] T.G. Meyers, J.P.F. Charpin, M.S. Tshela, The flow of a variable viscosity fluid between parallel plates with shear heating, Appl. Math. Model. 9 (2006) 799–815.
[20] S.S. Motsa, I.L. Animasaun, A new numerical investigation of some thermo–physical properties on unsteady MHD non-darcian flow past an impulsively started vertical surface, Therm. Sci. 19 (Suppl. 1) (2015) S249–S258.
[21] D. Pal, H. Mondal, Effects of temperature-dependent viscosity and variable thermal conductivity on MHD non-darcy mixed convective diffusion of species over a stretching sheet, J. Egypt. Math. Soc. 22 (2014) 123–133.
[22] N. Yacob, A. Ishak, I. Pop, Melting heat transfer in boundary layer stagnation–point flow towards a stretching/shrinking sheet in a micropolar fluid, Comput. Fluids 47 (2011) 16–21.
[23] A. Ishak, R. Nazar, N. Bachok, I. Pop, Melting heat transfer in steady laminar flow over a moving surface, Heat Mass Transf. 46 (2010) 463–468.
[24] D.E. Loper, An Analysis of Confined Magnetohydrodynamic Vortex Flows, (NASA Contractor Report NASA CR-646), National Aeronautics and Space Administration, Washington, 1966. LCCN 67060315, http://lccn.loc.gov/67060315
[25] G. Ahmadi, Self-similar solution of imcompressible micropolar boundary layer flow over a semi-infinite plate, Int. J. Eng. Sci. 14 (1976) 639–646.
[26] S. Mukhopadhyay, Effects of radiation and variable fluid viscosity on flow and heat transfer along a symmetric wedge, J. Appl. Fluid Mech. 2 (2009) 29–34.
[27] J. Charraudeau, Influence de gradients de properties physiques en convection force application au cas du tube, Int. J. Heat Mass Transf. 18 (1975) 87–95.
[28] M.M. Rahman, A.A. Mamun, M.A. Azim, M.A. Alim, Effects of temperature dependent thermal conductivity on magnetohydrodynamic (MHD) free convection flow along a vertical flat plate with heat conduction, Nonlinear Anal. 13 (2008) 13–524.
[29] I.L. Animasaun, Double diffusive unsteady convective micropolar flow past a vertical porous plate moving through binary mixture using modified boussinesq approximation, Ain Shams Eng. J. 7 (2016) 755–765.
[30] T.Y. Na, Computational Methods in Engineering Boundary Value Problems, Academic Press, New York, 1979.
[31] C.Y. Wang, Stagnation flow towards a shrinking sheet, Int. J. Non-Linear Mech. 43 (2008) 377–382.